

DEVICE: DEpth and VISual ConcEpts Aware Transformer for TextCaps

Dongsheng Xu, Qingbao Huang, *Member, IEEE*, Feng Shuang
Yi Cai, *Member, IEEE*

Abstract—Text-based image captioning is an important but under-explored task, aiming to generate descriptions containing visual objects and scene text. Recent studies have made encouraging progress, but they are still suffering from a lack of overall understanding of scenes and generating inaccurate captions. One possible reason is that current studies mainly focus on constructing the plane-level geometric relationship of scene text without depth information. This leads to insufficient scene text relational reasoning so that models may describe scene text inaccurately. The other possible reason is that existing methods fail to generate fine-grained descriptions of some visual objects. In addition, they may ignore essential visual objects, leading to the scene text belonging to these ignored objects not being utilized. To address the above issues, we propose a DEpth and VISual ConcEpts Aware Transformer (DEVICE) for TextCaps. Concretely, to construct three-dimensional geometric relations, we introduce depth information and propose a depth-enhanced feature updating module to ameliorate OCR token features. To generate more precise and comprehensive captions, we introduce semantic features of detected visual concepts as auxiliary information, and propose a semantic-guided alignment module to improve the model’s ability to utilize visual concepts. Our DEVICE is capable of generalizing scenes more comprehensively and boosting the accuracy of described visual entities. Sufficient experiments demonstrate the effectiveness of our proposed DEVICE, which outperforms state-of-the-art models on the TextCaps test set. Our code will be publicly available.

Index Terms—Text-based image captioning, multimodal representation, monocular depth estimation, visual object concepts.

I. INTRODUCTION

IMAGE captioning is one of the important tasks in the intersection of vision and language, which aims to automatically describe given images with natural language captions. Some recent studies have achieved superior performance and are even comparable to humans under certain circumstances [1]–[3]. However, these traditional image captioning models

Dongsheng Xu and Qingbao Huang are with the School of Electrical Engineering, the Guangxi Key Laboratory of Multimedia Communications and Network Technology, the Institute of Artificial Intelligence at Guangxi University, Nanning 530004, China (e-mail: 2112391059@st.gxu.edu.cn; qb-huang@gxu.edu.cn).

Feng Shuang is with the School of Electrical Engineering, Guangxi University, and with Guangxi Key Laboratory of Intelligent Control and Maintenance of Power Equipment, Nanning 530004, China (e-mail: fshuang@gxu.edu.cn).

Yi Cai is with the School of Software Engineering, South China University of Technology, Guangzhou 510006, China, and also with the Key Laboratory of Big Data and Intelligent Robot (SCUT), MOE of China, Guangzhou 510006, China (e-mail: ycai@scut.edu.cn).

This work has been submitted to the IEEE for possible publication. Copyright may be transferred without notice, after which this version may no longer be accessible.

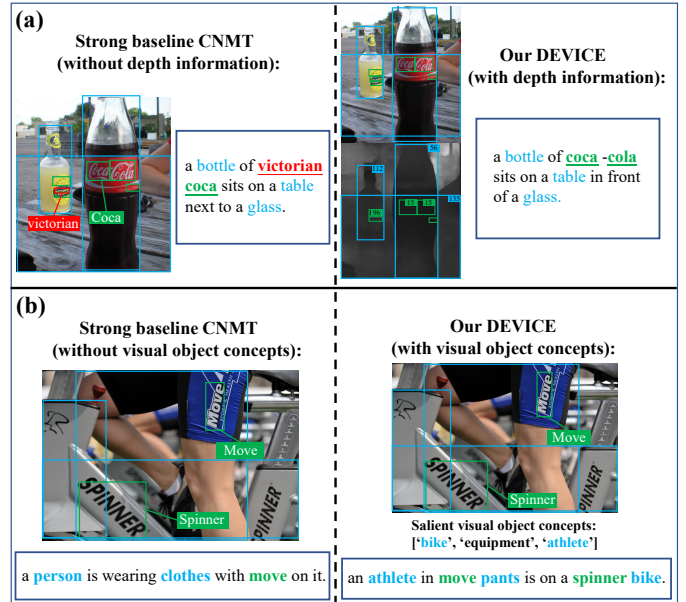


Fig. 1. Our DEVICE significantly improves the quality of captions. In Case a, with depth information and a depth-enhanced feature updating module, DEVICE correctly models 3D relationships between scene texts. With a salient visual object concepts extractor and a semantic-guided alignment module, DEVICE generates more accurate and comprehensive captions, cf. Case b. Scene text is represented in Green, and objects are represented in Blue.

perform unsatisfactorily when describing scenes containing text. As shown in Case (a) (cf. Fig. 1), “a bottle of Coca-Cola” is obviously specific than “a bottle”. To solve this defect, Sidorov *et al.* [4] propose text-based image captioning and collect a high-quality dataset TextCaps, in which captions contain scene text from the images.

To utilize the scene text in pictures, extracting Optical Character Recognition (OCR) tokens from given images is the precondition. M4C-Captioner [4] utilizes Rosetta [5] OCR system to obtain OCR tokens, and then employ a multimodal transformer directly to model the relationships between visual objects and OCR tokens. However, it is inappropriate to treat all OCR tokens equally, because only part of OCR tokens are crucial to the understanding of the scene. Wang *et al.* [6] creatively introduce a concept of OCR confidence to choose the noteworthy OCR tokens, which has greatly alleviated this issue. Then Wang *et al.* [7], [8] are committed to improving the spatial relationship construct methods for OCR tokens, which have been proven effective, and the proposed model LSTM-R [8] achieves the state-of-the-art performance. However, current

methods are not accurate and comprehensive enough when describing the scenes, which can be mainly manifested in the following two-fold.

Firstly, the real-world is three-dimensional (3D). However, current studies [4], [6]–[9] only exploit the spatial relationships of OCR tokens at the plane-level, which leads to visual location information being utilized incompletely, and even results in generating inaccurate scene text. As illustrated in the Case (a) of Fig. 1, CNMT [6] mistakenly regards “victorian” and “coca” as closely related OCR tokens in the same plane, which are irrelevant and actually one behind the other. Naturally, we consider that introducing depth information based on two-dimensional (2D) information can simulate real-world geometric information for improving the accuracy of scene text in captions.

Secondly, scenes contain abundant but complex visual entities (visual objects and scene text), existing methods suffer from coarse-grained descriptions of visual objects and the absence of crucial visual entities in captions. As shown in the Case (b) on the right of Fig. 1, CNMT [6] generates the coarse-grained word “person” for the visual object “athlete”. Besides, CNMT ignores an important entity “bike”, causing the OCR token “spinner” on it cannot be utilized effectively. One possible reason for the absence of “bike” is that the visual features of mutilated objects are not conducive to modeling. Intuitively, we consider that the semantic information of salient visual object concepts can alleviate coarse-grained and partial captioning.

To tackle the aforementioned issues, we propose a DEpth and VISual ConcEpts Aware Transformer (DEVICE) for TextCaps. It mainly comprises a reading module, a depth-enhanced feature updating module, a salient visual object concepts extractor, a semantic-guided alignment module, and a multimodal transformer. Concretely, in the reading module, we employ a monocular depth estimator BTS [10] to generate depth maps, then we extract depth values for visual objects and OCR tokens, respectively. The depth-enhanced feature updating module is designed to optimize the visual features of OCR tokens, which is beneficial for 3D geometry relationship construction. In the salient visual object concepts semantic extractor, we first employ a pre-trained visual-language model CLIP [11] as a filter to generate K concepts most related to the given picture. Then we adopt the semantic information of visual object concepts as augmentations to improve the overall expressiveness of our model. To utilize visual concepts more efficiently, we introduce the Semantic-guided Alignment Module to interact aligned visual concepts with corresponding scene text. Subsequent experiments in Section IV demonstrate the effectiveness of our proposed DEVICE.

Our main contributions can be summarized as follows:

- We propose a DEpth and VISual ConcEpts Aware Transformer (DEVICE) for TextCaps. DEVICE performs better than previous methods as it improves the accuracy and completeness of captions.
- We devise a Depth-enhanced Feature Updating Module (DeFUM) to enhance the 3D spatial relationship between OCR tokens, which effectively helps the model evaluate the relevance of OCR tokens. To our knowledge, we

are the first to apply depth information to the text-based image captioning task.

- We introduce semantic information of salient visual objects by the Visual Object Concepts Extractor (VOC), and we construct a Semantic-guided Alignment Module (SgAM) to improve the availability of visual concepts. Our DEVICE is capable of generating fine-grained objects in captions and better understanding holistic scenes.
- Our DEVICE outperforms the state-of-the-art models on the TextCaps test set, inspiringly boosting CIDEr-D from 100.8 to 110.0.

II. RELATED WORK

A. Text-based Image Captioning

Image captioning task has made a lot of progress in recent years [1], [12]–[15], but most of them perform poorly facing images with scene text. Text-based image captioning was naturally born to alleviate this problem, which was proposed by Sidorov *et al.* [4]. The authors introduced the Textcaps dataset and a multimodal Transformer-based [16] baseline model M4C-Captioner. The M4C-Captioner was modified from a Text-VQA [17]–[20] model M4C [21], and can encode both image and OCR tokens to generate more property captions. However, this paradigm suffers from a lack of diversity and information integrity. Zhang *et al.* [22] and Xu *et al.* [23] were committed to solving this problem by introducing additional captions. Although introducing multiple captions alleviates the problem of missing scene information, it is inherently hard to summarize the complex entities of a scene within one caption well. Apart from this, M4C-Captioner is less than satisfactory performed on Textcaps due to insufficient use of visual and semantic information of images. To distinguish misidentified OCR recognition results and pick out the crucial OCR tokens, Wang *et al.* [6] introduced confidence embedding and alleviated the adverse effects of inaccurate OCR tokens to a certain extent. Yang *et al.* [9] designed a pre-training model that can exploit OCR tokens and achieved strong results on multiple tasks, including text-based image captioning. Wang *et al.* [7], [8] and Tang *et al.* [24] employ the 2D spatial relationships to measure correlations between OCR tokens. Nevertheless, we find that simply leveraging two-dimensional spatial relationships may cause incorrect captions. Therefore, we ameliorate this problem by utilizing depth information.

B. Depth Information For Multimodal Tasks

Monocular depth estimation is a challenging problem of computer vision, whose purpose is to use depth values to measure the distance of objects relative to the camera [10], [25], [26]. With depth estimation technology, significant improvements have been achieved on many multimodal tasks [27]–[29]. In the visual question answer (VQA) task, Banerjee *et al.* [27] and Liu *et al.* [30] proved that exploiting three-dimensional relationships by depth information could enhance the spatial reasoning ability of VQA models. Apart from this, Qiu *et al.* [31] and Liao *et al.* [29] point out that ignoring the depth information could tremendously place restrictions on applications of scene change captioning in the real world.

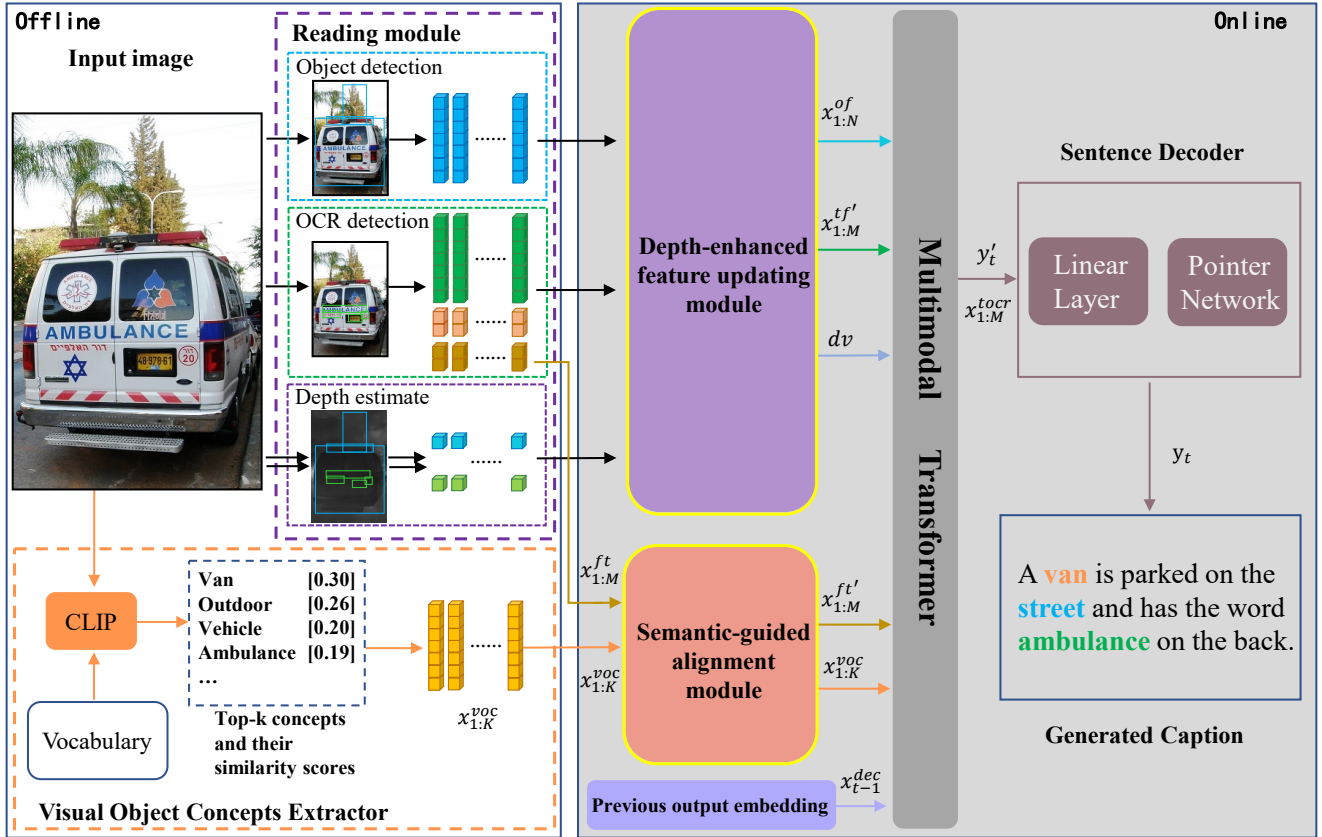


Fig. 2. Overview of our DEpth and Visual ConcEpts Aware Transformer for TextCaps (DEVICE). In the reading module, we first extract visual objects and OCR tokens along with their depth values. Then a depth-enhanced feature updating module is constructed to enhance OCR appearance features with the help of depth values. After that, DEVICE utilizes depth information and plane geometry relationships to construct 3D positional relationships. Semantic information of salient visual object concepts promotes fine-grained and holistic captioning, and the proposed semantic-guided alignment module improves the model’s efficiency to utilize visual concepts. Words in **Blue**, **Green** and **Orange** represent objects, scene text, and visual concepts, respectively.

At the same time, we notice that text-based image captioning is facing the same problem. Therefore, we improve the 3D relationship modeling method to apply in text-based image captioning effectively.

III. APPROACH

A. Overview

Given an image I , text-based image captioning models aim to automatically generate caption $C = [y_0, y_1, \dots, y_n]$ based on scene text S in the image.

As depicted in Fig. 2, our DEVICE mainly consists of a reading module, a depth-enhanced feature updating module, a salient visual object concepts extractor, a semantic-guided alignment module, a multimodal transformer, and a sentence decoder. Concretely, the input image is first put into an object detector and two OCR detectors to extract N visual objects and M OCR tokens along with their 2D regional coordinates. Then we utilize a pre-trained depth estimation model to generate the pixel-level depth map D and construct 3D coordinates of visual entities. After that, we update the visual features of OCR tokens with the depth-enhanced feature updating module. Depth information is included in the coordinates of both scene text and objects, hence the multimodal transformer could establish 3D relations between visual entities. Meanwhile, to

generate salient visual object concepts for each image, we employ a pre-trained cross-modal tool CLIP [11] to match the top- K related visual concepts (e.g., “Van” and “Vehicle”) in vocabulary. Then we propose the semantic-guided alignment module to integrate the information of aligned visual concepts into the representation of relevant OCR tokens. Ultimately, the multimodal transformer and sentence decoder generate captions in the auto-regressive paradigm.

B. Multimodal Embedding

First of all, we exploit pre-trained Faster R-CNN [32] model to get the bounding box coordinates $\{b_n^{obj}\}_{n=1:N}$ of objects $\{a_n^{obj}\}_{n=1:N}$. To ensure high quality OCR tokens, following LSTM-R [8], we apply external OCR systems [5], [33] to obtain both OCR tokens $\{a_m^{ocr}\}_{m=1:M}$ and corresponding bounding box coordinates $\{b_m^{ocr}\}_{m=1:M}$, respectively. After that, we extract the d -dim appearance features $\{x_n^{of}\}_{n=1:N}$ of objects and appearance features $\{x_m^{tf}\}_{m=1:M}$ of OCR tokens by Faster R-CNN [32]. To generate depth maps of images in the TextCaps dataset, we utilize a monocular depth estimation model BTS [10].

Depth values. To measure the relative distance of objects and OCR tokens to the observer, we employ a pre-trained depth estimation model BTS [10] to generate depth maps.

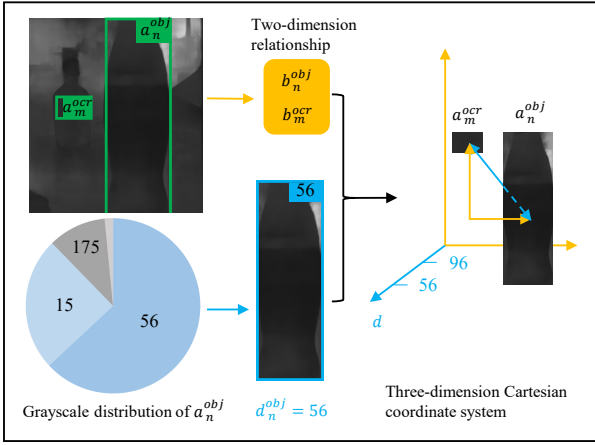


Fig. 3. Illustrations for the process of getting the depth values and 3D geometric relationship modeling. The pie chart represents the gray value distribution of object a_n^{obj} . We take the gray values with the highest proportion as the depth value (0 means nearest) of object a_n^{obj} and OCR token a_m^{ocr} . b_n^{obj} and b_m^{ocr} denote bounding boxes of a_n^{obj} and a_m^{ocr} , respectively. With depth information, relationships between visual entities become more clear.

Subsequently, we unify the values of the depth maps to the range of 0 to 255. For object a_n^{obj} and OCR token a_m^{ocr} , we count the grayscale distribution of bounding box region of a_n^{obj} and a_m^{ocr} in the depth map at pixel scale. We take the gray values with the highest frequency as the depth values for object a_n^{obj} and OCR token a_m^{ocr} (cf. Fig. 3). We denote $\{dv_n^{obj}\}_{n=1:N}$ as the depth values for $\{a_n^{obj}\}_{n=1:N}$ and $\{dv_m^{ocr}\}_{m=1:M}$ for $\{a_m^{ocr}\}_{m=1:M}$, respectively.

Embedding of objects. To measure the relationship between visual entities more effectively, we incorporate depth information into object features. For the object a_n^{obj} , we denote its 2D geometry coordinate by $b_n^{obj} = [x^{tl}/W; y^{tl}/H; x^{br}/W; y^{br}/H]$, where x^{tl} and y^{tl} represent the coordinates of the upper left corner of object a_n^{obj} , x^{br} and y^{br} represent the coordinates of the bottom right corner of object a_n^{obj} , respectively. Then we denote the 3D spatial location feature of a_n^{obj} by $x_n^{os} = [b_n^{obj}; dv_n^{obj}/255]$. The embedding of object a_n^{obj} is calculated as

$$x_n^{obj} = LN(W_{of}x_n^{of}) + LN(W_s x_n^{os}), \quad (1)$$

where $W_{fr} \in \mathbb{R}^{t \times d}$ and $W_s \in \mathbb{R}^{t \times 5}$, t represents the dimension of common space in multimodal transformer, and LN represents layer normalization.

Embedding of OCR tokens. Unlike objects, OCR tokens not only contain rich visual clues but also contain rich semantic information. To get rich representations of OCR tokens, following Hu *et al.* [21] and Sidorov *et al.* [4], we apply FastText [34] to extract the 300-dim subword feature x_m^{ft} for OCR token a_m^{ocr} , and employ PHOC (Pyramidal Histogram of Characters) [35] to extract 604-dim character-level feature x_m^{ph} for a_m^{ocr} . Similarly, the spatial location of a_m^{ocr} is denoted as $x_m^{ts} = [b_m^{ocr}; dv_m^{ocr}/255]$, where $b_m^{ocr} = [x^{tl}/W; y^{tl}/H; x^{br}/W; y^{br}/H]$. To better fuse the three-dimensional relative spatial relationships into OCR features, we propose a Depth-enhanced Feature Updating Module (DeFUM, cf. Section III-C). In the real world, scene texts are

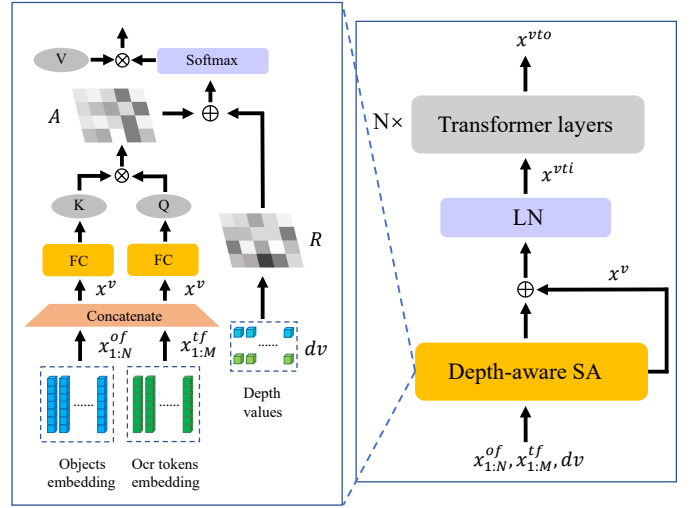


Fig. 4. Illustration of the Depth-enhanced Feature Updating Module (DeFUM), which consists of a depth-aware self-attention module and N layers of transformer encoder. The DeFUM could effectively enhance the appearance features of OCR tokens with the help of depth information, which is conducive to constructing the three-dimensional geometric relationships and improving the accuracy of captions.

attached to the surface of objects. We consider that visual features of objects can help model the visual relationship of OCR tokens. For example, if several different OCR tokens are on the same object, then these OCR tokens are likely to have a strong correlation. Therefore we fed the OCR token appearance features $x_{1:M}^{tf}$ into DeFUM along with object appearance features $x_{1:N}^{of}$, we can get the depth-enhanced OCR appearance feature $x_{1:M}^{tf'}$:

$$x_{1:M}^{tf'} = DeFUM(x_{1:N}^{of}, x_{1:M}^{tf}, dv_{1:N}^{obj}, dv_{1:M}^{ocr}), \quad (2)$$

where $dv_{1:N}^{obj} \in \mathbb{R}^{N \times 1}$ and $dv_{1:M}^{ocr} \in \mathbb{R}^{M \times 1}$, respectively. Considering the gap between visual features and semantic features, we do not update FastText and PHOC features (semantic embeddings). Then we utilize the Semantic-guided Alignment Module (SgAM, cf. Section III-E) to integrate aligned visual concept information into the semantic representation of relevant OCR tokens

$$x_{1:M}^{ft'} = SgAM(FT(a_{1:K}^{voc}), x_{1:M}^{ft}), \quad (3)$$

where $x_{1:M}^{ft'}$ and $x_{1:M}^{ft} \in \mathbb{R}^{M \times 300}$, $FT(a_k^{voc})$ represent the FastText embedding of visual concept a_k^{voc} (cf. Section III-D).

Following Wang *et al.* [6], we adopt confidence features of detected OCR tokens $\{x_m^{conf}\}_{m=1:M}$ due to some OCR tokens may be amiss. The final embedding of OCR token a_m^{ocr} could be calculated by

$$x_m^{ocr} = LN(W_{tf}x_m^{tf'} + W_{ft}x_m^{ft'} + W_{ph}x_m^{ph}) + LN(W_s x_m^{ts}) + LN(W_{conf}x_m^{conf}), \quad (4)$$

where $W_{tf} \in \mathbb{R}^{t \times d}$, $W_{ft} \in \mathbb{R}^{t \times 300}$, $W_{ph} \in \mathbb{R}^{t \times 604}$, $W_s \in \mathbb{R}^{t \times 5}$ and $W_{conf} \in \mathbb{R}^{t \times 1}$ are learnable parameters, and LN represents layer normalization.

C. Depth-enhanced Feature Updating Module

Unlike other multimodal tasks, such as VQA, which require high-quality relationships between objects, text-based image captioning requires models with stronger scene text relationship modeling capabilities. Therefore the quality of the OCR token features is more critical to the generated captions. For this reason, we propose the DeFUM to enhance the OCR appearance features $\{x_m^{tf}\}_{m=1:M}$ with the help of depth information. Intuitively, we consider that object features can play the role of a bridge linking its adjacent scene text. Therefore, we first obtain appearance embedding x^v of visual entities by concatenating the visual features $\{x_n^{of}\}_{n=1:N}$ of objects $\{a_n^{obj}\}_{n=1:N}$ and the visual features $\{x_m^{tf}\}_{m=1:M}$ of OCR tokens $\{a_m^{ocr}\}_{m=1:M}$:

$$x^v = \text{Concat}(x_{1:N}^{of}, x_{1:M}^{tf}), \quad (5)$$

where $x^v \in \mathbb{R}^{(m+n) \times d}$. Subsequently, we calculate the query Q , key K , and value V as follows:

$$\begin{cases} Q = x^v W_Q \\ K = x^v W_K, \\ V = x^v W_V \end{cases} \quad (6)$$

where query $Q \in \mathbb{R}^{(m+n) \times d}$, key $K \in \mathbb{R}^{(m+n) \times d}$, value $V \in \mathbb{R}^{(m+n) \times d}$. Then, we can obtain the attention weights matrix A by:

$$A = \frac{QK^T}{\sqrt{d}}, \quad (7)$$

where $K \in \mathbb{R}^{(m+n) \times (m+n)}$. To measure the relative depth between different visual entities, we calculate the relative depth score of x_i^v and x_j^v by

$$R_{i,j} = \log\left(\frac{dv_j}{dv_i}\right), \quad (8)$$

where $dv = \text{Concat}(dv^{obj}, dv^{ocr})$ and the relative depth map $R \in \mathbb{R}^{(m+n) \times (m+n)}$. Then the output of Depth-aware Self-Attention module (cf. Fig. 4) is updated by

$$x^{vti} = \text{LN}(x^v + \text{softmax}(A + R)V), \quad (9)$$

where the depth-aware visual feature $x^{vti} \in \mathbb{R}^{(m+n) \times d}$, LN denotes layer normalization. Eventually, x^{vti} is fed into N layers of transformer [16] to update appearance features with depth information

$$x^{vto} = \text{transformer}(x^{vti}), \quad (10)$$

where the depth-enhanced appearance feature $x^{vto} \in \mathbb{R}^{(m+n) \times d}$ ($x^{vto} = [x^{of'}, x^{tf'}]$), $x^{of'} \in \mathbb{R}^{n \times d}$, $x^{tf'} \in \mathbb{R}^{m \times d}$, respectively.

D. Salient Visual Object Concepts Extractor

To improve the modeling ability of the multimodal transformer to the scene objects, avoid the lack of vital objects, and generate more accurate captions, we propose a visual object concepts extractor to introduce semantic information of visual object concepts. Specifically, we employ a pre-trained model CLIP [11] to match 15 object concepts related to the given image from vocabulary. Then we sort them by similarity score

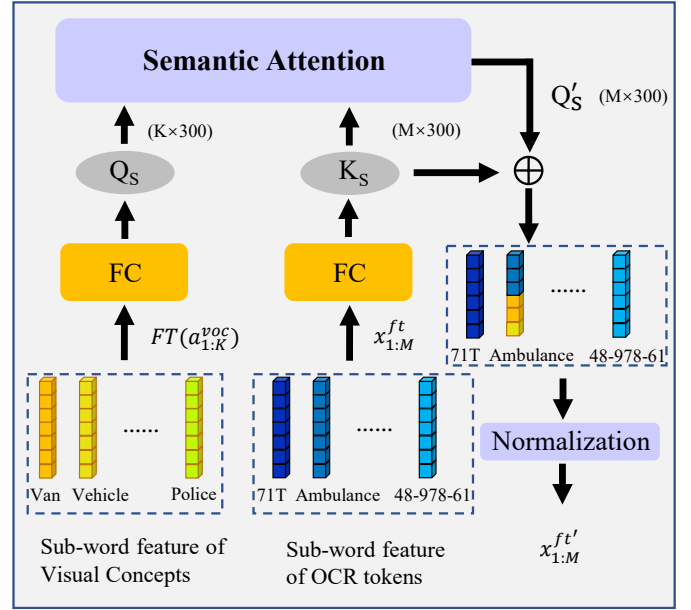


Fig. 5. Illustration of the Semantic-guided Alignment Module (SgAM), which utilizes semantic attention to transfer the information of visual concepts to semantically aligned OCR Tokens’ sub-word embedding. This operation is capable of making model emphasize visual concepts that are highly relevant to the scene text. Besides, SgAM helps multimodal transformer roughly model the spatial location of semantically aligned visual concepts.

and take the top- K as visual object concepts. Visual object concepts and similarity score are represented as $\{a_k^{voc}\}_{k=1:K}$ and $\{a_k^{score}\}_{k=1:K}$. The embedding of visual object concepts are calculated as follows:

$$x_k^{voc} = \text{LN}(W_{voc}FT(a_k^{voc})) + \text{LN}(W_{score}a_k^{score}), \quad (11)$$

where $FT(a_k^{voc})$ means the FastText [34] embedding of a_k^{voc} , $W_{voc} \in \mathbb{R}^{t \times 300}$ and $W_{score} \in \mathbb{R}^{t \times 1}$.

E. Semantic-guided Alignment Module

CLIP [11] is a large-scale pre-trained model based on contrastive learning, whose powerful representation ability has been fully demonstrated by the application of downstream tasks [36], [37]. However, CLIP embeds the whole image and sentence into textual and visual representations, which makes it difficult for CLIP’s image encoder to capture fine-grained features [38]. Therefore, it is hard to ground the area depicted by these visual concepts, which may prevent the model from effectively understanding the representations of visual concepts. In addition, to avoid the introduction of out-of-domain words, we do not use words that are not included in the vocabulary provided by M4C-Captioner [4] for visual object concept extraction. Accordingly, a small part of visual concepts may be invalid, because there may be less than K words related to the given image in the limited vocabulary.

To alleviate the above potential problems, we propose a Semantic-guided Alignment Module (SgAM, cf. Fig. 5). The sub-word embedding extracting model FastText is trained on Wikipedia data. Therefore, related words (e.g., Van and Vehicle) have relatively high semantic similarity. Taking advantage of this factor, we integrate semantic information of visual

concepts into related OCR tokens features. The semantic integration operation not only helps the model distinguish visual concepts related to OCR tokens but also roughly models the spatial position of some visual concepts during the interaction with spatial position information of OCR tokens in the multimodal transformer.

Concretely, we first convert FastText embedding of visual concepts $FT(a_{1:K}^{voc})$ to query Q_S and convert FastText embedding of OCR tokens $x_{1:M}^{ft}$ to value K_S , respectively:

$$\begin{cases} Q_S = FT(a_{1:K}^{voc})W_{Q_S} \\ K_S = x_{1:M}^{ft}W_{K_S}, \end{cases} \quad (12)$$

where $FT(a_{1:K}^{voc}) \in \mathbb{R}^{K \times 300}$, $x_{1:M}^{ft} \in \mathbb{R}^{M \times 300}$, while W_{Q_S} and $W_{K_S} \in \mathbb{R}^{300 \times 300}$.

Subsequently, we adopt semantic attention to interact semantic information of visual concepts and OCR tokens

$$Q'_S = softmax(\frac{Q_S K_S^T}{\sqrt{d_s}})^T FT(a_{1:K}^{voc}), \quad (13)$$

where $Q'_S \in \mathbb{R}^{M \times 300}$. Then we can get the final semantic embedding $x_{1:M}^{ft'}$ of OCR tokens

$$x_{1:M}^{ft'} = L2Norm(x_{1:M}^{ft} + Q'_S), \quad (14)$$

where $x_{1:M}^{ft'}$ and $x_{1:M}^{ft} \in \mathbb{R}^{M \times 300}$, while $L2Norm$ represents L2 Normalization.

F. Reasoning and Generation Module

Following Sidorov *et al.* [4], we adopt a multimodal transformer to encode all the obtained embeddings. Considering most OCR tokens (e.g., ‘‘coca’’ and ‘‘spinner’’ in Fig. 1) are not common words, therefore it is not appropriate to generate captions based on a fixed vocabulary. Following M4C-Captioner [4], we utilize two classifiers for common vocabulary and candidate OCR tokens separately to generate words. Overall, multimodal transformer models multimodal embedding and generates common words y'_t . Afterward, a dynamic pointer network [39] is employed to generate final words y_t :

$$y'_t, x_{1:M}^{toocr} = mmt(x_{1:N}^{obj}, x_{1:M}^{ocr}, x_{1:K}^{voc}, x_{t-1}^{dec}), \quad (15)$$

where mmt represents multimodal transformer, $x_{1:M}^{toocr}$ indicates the feature of x_m^{ocr} updated by mmt , and x_{t-1}^{dec} is the embedding of previous output y'_{t-1} , respectively. Eventually, the dynamic pointer network makes the final prediction from the common word in the fixed vocabulary and the special words $x_{1:m}^{toocr}$ from OCR tokens:

$$y_t = argmax([l_m^w(y'_t), PN(y'_t, x_{1:m}^{toocr})]), \quad (16)$$

where $l_m^w(\cdot)$ denotes a linear classifier for fixed common vocabulary, $PN(\cdot)$ denotes pointer network, and the caption C consists of predicted words y_0, \dots, y_t . We train our model by optimizing the Cross-Entropy loss:

$$L(\theta) = - \sum_{t=1}^T \log(\hat{y}_t | y_{1:t-1}, x_{1:m}^{toocr}), \quad (17)$$

where \hat{y}_t is the corresponding token in the ground truth.

IV. EXPERIMENTS

A. Dataset and Settings

Dataset and evaluation metrics. The TextCaps dataset [4] is constructed for text-based image captioning, which contains 28408 images with 5 captions per image. The training, validation, and test set contain 21953, 3166, and 3289 images, respectively. For evaluation metrics, we choose five widely used evaluation metrics for image captioning, i.e., BLEU-4 [40], ROUGE-L [41], METEOR [42], SPICE [43], and CIDEr-D [44]. Following Sidorov *et al.* [4], we focus on the CIDEr-D metric when comparing different methods, because CIDEr-D has a high correlation with human evaluation scores and puts more weight on informative special tokens (e.g., OCR tokens) in the captions.

Settings and implementation details. To improve the robustness of the OCR system and increase the accuracy of detected OCR tokens, we employ the Rosetta OCR system [5] and Google OCR system [33] following Wang *et al.* [8]. The number of OCR tokens for each image is limited to 80 at most. We extract 100 object appearance features for each picture, the dimension d of appearance features is 2048, and the dimension t of common embedding space in the multimodal transformer is 768. The maximum generation length is 30. DeFUM contains two layers of transformer encoder in our experiments, we set the layer number of the multimodal transformer to 4 and the number of self-attention heads to 12. We adopt default settings for other parameters following BERT-BASE [47]. The fixed common vocabulary has 6736 words. To get visual object concepts, we filter top- k ($k = 5$ in our implement) visual concepts from the vocabulary by CLIP [11]. We retain the similarity score given by CLIP as a reference for measuring the relevance of visual concepts to the image. To get the confidence of OCR tokens, for those OCR tokens detected by Rosetta, we adopted the confidence provided by Wang *et al.* [6]. For those OCR tokens that only appear in one OCR system, we set the confidence to 0.9.

We train the model for about 5 epochs (9000 iterations) on a single 3090 Ti GPU, and the batch size is 64. We adapt Adam [48] optimizer, the initial learning rate is $1e-4$ and is declined to 0.1 times at 7000 iterations. We monitored the CIDEr-D metric to choose the best model and evaluate it on both the validation set and test set. All the experimental results are computed by Eval AI online platform submissions.

B. Experimental Results

Compared models. We make comparisons with other models in Table I and Table II. **M4C-Captioner** [4], **SS-Baseline** [45], **CNMT** [6], and **ACGs-Captioner** [23] are Transformer-based strong baseline models. **MMA-SR** [7], **MAGIC** [22], **OMOT** [24], and **LSTM-R** [8] are LSTM-based strong baseline models.

- **Up-Down** [1] and **AOA** [13] are widely used image captioning models. Both of them are trained and inferred without OCR tokens.
- **M4C-Captioner** [4] is a Transformer-based strong baseline model, which firstly introduces the OCR system into the TextCaps dataset.

TABLE I

COMPARISON OF OUR PERFORMANCE WITH OTHER BASELINE MODELS ON THE TEXTCAPS VALIDATION SET. TAP[†] AND CONCAP[†] ARE PRE-TRAINED MODELS. OUR DEVICE OUTPERFORMS STATE-OF-THE-ART MODELS ON METOR, ROUGE-L, SPICE, AND CIDER-D.

Model	BLEU-4	METEOR	ROUGE-L	SPICE	CIDER-D
Up-Down (CVPR 2018) [1]	20.1	17.8	42.9	11.7	41.9
AoA (ICCV 2019) [13]	20.4	18.9	42.9	13.2	42.7
M4C-Captioner (ECCV 2020) [4]	23.3	22.0	46.2	15.6	89.6
MMA-SR (ACM MM 2020) [7]	24.6	23.0	47.3	16.2	98.0
SS-Baseline (AAAI 2021) [45]	24.9	22.7	47.2	15.7	98.8
CNMT (AAAI 2021) [6]	24.8	23.0	47.1	16.3	101.7
ACGs-Captioner (CVPR 2021) [23]	24.7	22.5	47.1	15.9	95.5
MAGIC (AAAI 2022) [22]	22.2	20.5	42.3	13.8	76.6
OMOT (ICMR 2022) [24]	26.4	22.2	47.5	14.9	95.1
LSTM-R (CVPR 2021) [8]	27.9	23.7	49.1	16.6	109.3
DEVICE (Ours)	27.6	24.6	49.3	17.7	117.1
M4C-Captioner(w/ GT OCRs) [4]	26.0	23.2	47.8	16.2	104.3
TAP [†] (CVPR 2021) [9]	25.8	23.8	47.9	17.1	109.2
ConCap [†] (AAAI 2023) [46]	31.3	-	-	-	116.7

TABLE II

COMPARISON OF OUR PERFORMANCE WITH OTHER BASELINE MODELS ON THE TEXTCAPS TEST SET. OUR DEVICE OUTPERFORMS STATE-OF-THE-ART MODELS ON ALL METRICS, NOTABLY BOOSTING CIDER-D FROM 100.8 TO 110.0.

Model	BLEU-4	METEOR	ROUGE-L	SPICE	CIDER-D
Up-Down (CVPR 2018) [1]	14.9	15.2	39.9	8.8	33.8
AoA (ICCV 2019) [13]	15.9	16.6	40.4	10.5	34.6
M4C-Captioner (ECCV 2020) [4]	18.9	19.8	43.2	12.8	81.0
MMA-SR (ACM MM 2020) [7]	19.8	20.6	44.0	13.2	88.0
SS-Baseline (AAAI 2021) [45]	20.2	20.3	44.2	12.8	89.6
CNMT (AAAI 2021) [6]	20.0	20.8	44.4	13.4	93.0
ACGs-Captioner (CVPR 2021) [23]	20.7	20.7	44.6	13.4	87.4
OMOT (ICMR 2022) [24]	21.2	19.6	44.4	12.1	84.9
LSTM-R (CVPR 2021) [8]	22.9	21.3	46.1	13.8	100.8
DEVICE (Ours)	23.1	22.5	46.7	15.0	110.0
M4C-Captioner(w/ GT OCRs) [4]	21.3	21.1	45.0	13.5	97.2
TAP [†] (CVPR 2021) [9]	21.9	21.8	45.6	14.6	103.2
ConCap [†] (AAAI 2023) [46]	27.4	-	-	-	105.6
Human [4]	24.4	26.1	47.0	18.8	125.5

- **SS-Baseline** [45] introduces attention branches for visual and linguistic features of scene text.
- **CNMT** [6] is the state-of-the-art Transformer-based model, which adopts the confidence of scene text, and introduces a non-repetitive generation paradigm.
- **ACGs-Captioner** [23] introduces the anchor-centred graph (ACG), and based on different ACGs generate diverse captions.
- **MAGIC** [22] constructs multiple multimodal relational graphs to improve the diversity of captions and employs a cascaded generative adversarial network to generate unpaired captions.
- **MMA-SR** [7] is the first to explore sufficient two-dimensional spatial relationships between text tokens, and the model performance is remarkable.
- **OMOT** [24] explores the master object for each OCR token, then builds scene graphs based on these master objects.
- **LSTM-R** [8] is the state-of-the-art LSTM-based model, which expands the two-dimensional geometric relationship measurement of OCR tokens on the basis of MMA-SR, such as IOU. LSTM-R can select high-quality OCR

tokens with the help of a relation-aware pointer network.

- **TAP[†]** [9] is a text-aware pre-trained model, which is trained on TextVQA [17], STVQA [49], TextCaps [4], and OCR-CC [9].
- **ConCap[†]** [46] is a pre-trained image captioning framework, which caption style can be controlled by prompts. ConCap[†] is pre-trained on Visual Genome [50], COCO [51], Conceptual Caption [52], SBU Captions [53], and a filtered version of LAION [54].
- **M4C-Captioner (w/ GT OCRs)** [4] indicates **M4C-Captioner** takes ground truth OCR tokens as input and evaluates on a subset of the TextCaps test set.
- **Human** [4] represents human-generated captions.

Main results on the TextCaps validation set. The comparisons on the validation set between our DEVICE and other models are shown in Table I. Traditional methods UP-Down and AOA perform less well than other models with OCR tokens due to they cannot generate scene text. CNMT proves the effectiveness of confidence embedding and repetition mask, which improves CIDER-D from 89.6 to 101.7 compared with M4C-Captioner. LSTM-R constructs sufficient 2D spatial relations and boosts all metrics significantly. By incorporating

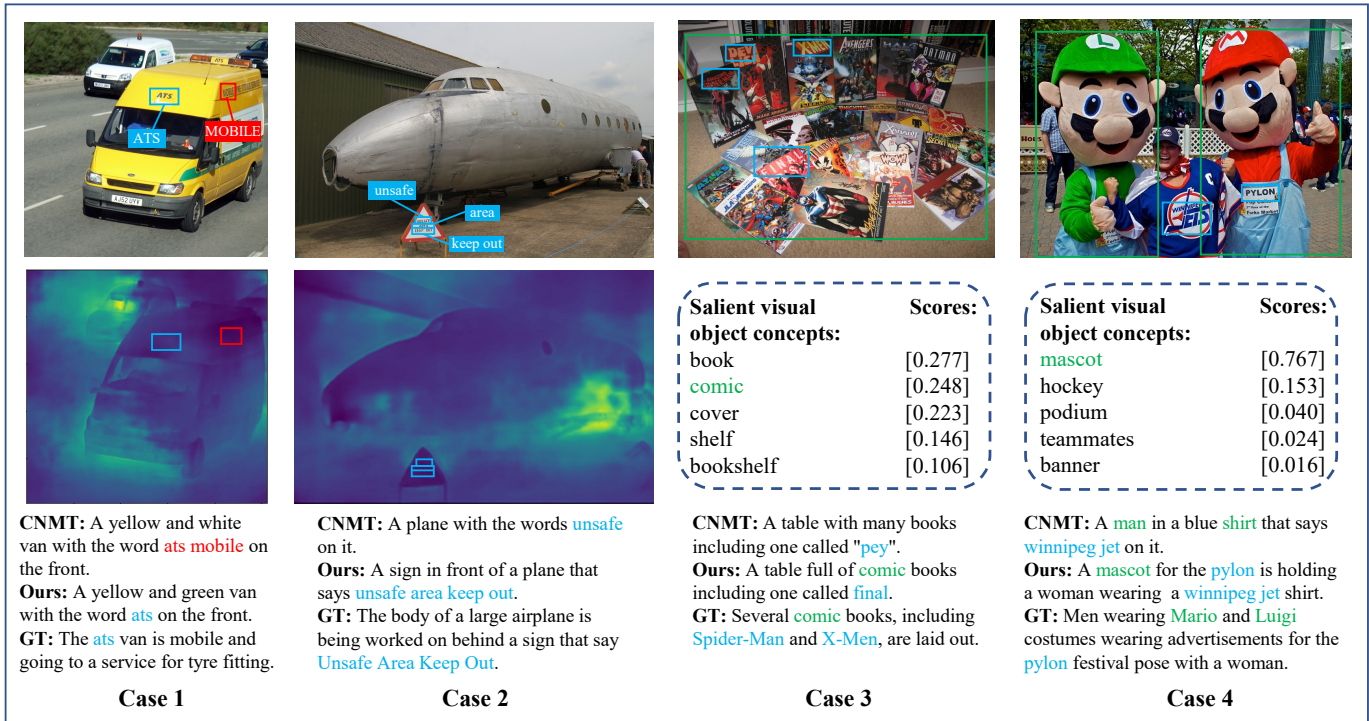


Fig. 6. Example of captions generated by strong baseline CNMT [6], DEVICE, and GT (ground truth). Red indicates inappropriate sense text generated by CNMT. The depth maps and visual object concepts are displayed in the middle. The score of visual object concepts measures how similar these concepts are to the image. Blue indicates scene text and Green indicates visual object concepts.

TABLE III
COMPARISON OF ITERATIONS AND TIME OF DEVICE AND OTHER BASELINE MODELS REQUIRED TO CONVERGE TO THE OPTIMAL CIDER.

Model	Batch Size	Iterations/epochs	Time
M4C-Captioner	128	12000/14	11h
CNMT	128	12000/14	12h
ACGs-Captioner	128	12000/14	12h
SS-Baseline	128	15000/17	14h
LSTM-R	50	-/30	-
DEVICE(w/o SgAM)	64	12000/7	11h
DEVICE	64	9000/5	8h
TAP [†]	-	480000/-	-
ConCap [†]	2880	-/37	-

TABLE IV
ABLATION OF EACH MODULE IN DEVICE ON THE TEXTCAPS VALIDATION SET. GOOGLE DENOTES GOOGLE OCR SYSTEM, DI DENOTES DEPTH INFORMATION, DEFUM REPRESENTS THE DEPTH-ENHANCED FEATURE UPDATING MODULE, VOC INDICATES SEMANTIC INFORMATION OF VISUAL OBJECT CONCEPTS, AND SgAM REPRESENTS SEMANTIC-GUIDED ALIGNMENT MODULE.

	Google	DI	DeFUM	VOC	SgAM	BLEU-4	CIDEr-D
1						24.5	101.5
2	✓					24.9	105.3
3	✓	✓				25.6	109.8
4	✓	✓	✓			26.1	113.9
5	✓			✓		26.3	112.4
6	✓			✓	✓	26.5	114.4
7	✓	✓	✓	✓		27.4	115.9
8	✓	✓	✓	✓	✓	27.6	117.1

depth information and semantic information of visual object concepts with transformer, compared with SOTA model LSTM-R [8], our DEVICE improves the performance on METEOR, SPICE, CIDEr-D by 0.9, 1.1, and 7.8, respectively. The performance of DEVICE on BLEU-4 ranks second only to LSTM-R (0.3 below). Note that LSTM-R has cleaned the training captions by removing the undetected OCR symbols, which increases BLEU-4 by 0.6 [8]. For a fair comparison, we train our model with raw captions provided by TextCaps [4], following the majority [4], [6], [9], [45]. Moreover, CIDEr-D and METEOR have the highest correlation with human scores [4], which shows that DEVICE significantly outperforms other baseline models from a human perspective. The performance of our model on the TextCaps validation set demonstrates the effectiveness of our DEVICE.

Main results on the TextCaps test set. Compared with

LSTM-R, our model shows superiority on the TextCaps test set, which gains rises of 0.2, 1.2, 0.6, 1.2, 9.2 on BLEU-4, METEOR, ROUGE-L, SPICE, CIDEr-D, respectively. Significantly, the inspiring improvement on the CIDEr-D shows that our DEVICE generates more accurate scene text. The results of m4c-captioner (w/ GT OCRs) [4] are evaluated on a subset of the TextCaps test set, excluding those samples without OCR annotations. DEVICE outperforms m4c-captioner(w/ GT OCRs) verifies that our DEVICE is capable of compensating the negative impact of the error of OCR systems to some extent. Encouragingly, our model outperforms the pre-trained model TAP[†] on all metrics, demonstrating that DEVICE utilizes limited training data more efficiently. The BLEU-4 score of ConCap[†] is 27.3, which shows that ConCap[†] has learned human language ability well from the large-scale corpus.

TABLE V
ANALYSIS OF VISUAL OBJECT CONCEPTS NUMBER K ON VALIDATION SET. VOC INDICATES VISUAL OBJECT CONCEPTS.

Model	Number of VOC	CIDEr-D
DEVICE	$K = 3$	115.9 ↓1.2
DEVICE	$K = 5$	117.1
DEVICE	$K = 8$	116.5 ↓0.6
DEVICE	$K = 10$	116.1 ↓1.0

However, DEVICE outperforms ConCap[†] on CIDEr-D, which shows that the scene text in the captions generated by DEVICE is of higher quality. Finally, the gap between machines and humans narrows on the text-based image captioning task.

Analysis of model convergence speed. In our experiments, we find that the SgAM module can significantly improve the model’s converge speed, and achieve better results with fewer iterations. In Table III, we list different models’ iteration numbers and training epochs when achieving the optimal CIDEr-D. With SgAM, the required training time for DEVICE is reduced from 11 hours to 8 hours. This proves that semantic attention can help the multimodal transformer quickly select effective visual entities. M4C-Captioner, CNMT, ACGs-Captioner, and SS-Baseline are trained on 2 RTX 3090 Ti GPUs in Table III.

C. Ablation Studies

To analyze the respective effects of each module on the model performance, we conduct ablation experiments, as shown in Table IV. Comparing Line 1 and Line 2, CIDEr-D is boosted from 101.5 to 105.3. It is evident that more affluent and more accurate OCR tokens positively impact the model performance. While the improvement on BLEU-4 is relatively moderate, we think one reason may be that BLEU-4 treats all matched words equally, but CIDEr-D pays more attention to OCR tokens. Line 2 and 3 prove that simply concatenating depth values with two-dimensional space coordinates boosts the performance substantially, which increases BLEU-4 by 0.7 and CIDEr-D by 4.5, respectively. Comparing Line 3 and 4, we find that updating the appearance features of OCR tokens under the supervision of depth information boosts all metrics. The significant improvements between Line 4 and 7 demonstrate the effectiveness of visual object concepts’ semantic information, which boosts BLEU-4 by 1.3 and CIDEr-D by 2.0, respectively. The introduction of SgAM reduces the iterations for the model to converge to the optimum, and improves the model’s performance on CIDEr-D by 2.0, respectively. More remarkably, the total increase ratio of CIDEr-D is 11.8 and BLEU-4 is 2.7. This demonstrates that all modules work together very efficiently.

We also evaluate the influences of the number K of visual object concepts on the TextCaps validation (cf. Table V). The experimental results indicate that some salient visual object concepts may be missed when K is less than 5. Meanwhile, irrelevant visual concepts may be retrieved when K is larger than 7. Therefore, we set K to 5.



Fig. 7. Negative samples of CNMT and DEVICE on the TextCaps validation set. The objects are inside the Green bounding boxes, the OCR tokens are inside the Blue bounding boxes. GT represents the Ground Truth.

D. Qualitative Analysis

We show some cases which are generated by CNMT [6] and DEVICE on the TextCaps validation set in Fig. 6, where “GT” means ground truth. We pick CNMT [6] for comparison because our geometric relationship construction methods are the same except for depth, and both are Transformer-based structures. Case 1 and Case 2 demonstrate the effectiveness of visual entities’ 3D spatial relationship modeling ability. Case 3 and 4 illustrate the influences of effectively utilize visual object concepts by SgAM. In Case 1, CNMT mistakenly takes “ats” and “mobile” as tokens in the same plane and connects them incorrectly. By introducing 3D geometric relationship, our DEVICE generates accurate scene text. In Case 2, CNMT incompletely represents the text in the sign and confuses the positional relationship between the airplane and the text on the sign. DEVICE enhances the correlation of scene text on the warning sign and clarifies the spatial relationship between visual entities by introducing 3D geometric relationships. For Case 3, CNMT only generates relatively coarse-grained words such as “many books”. In contrast, with the help of semantic information of visual object concepts and SgAM, DEVICE is capable of generating more accurate words “comic books”, like human. In the last case, unlike CNMT, which ignores the visual object “mascots”, DEVICE generates a more comprehensive description, enabling rational use of scene text “pylon”. The aforementioned cases demonstrate the effectiveness of DEVICE well.

However, in Case 4, we can see the gap between our DEVICE and human, we consider one possible reason is that humans have common knowledge. Although adopting CLIP [11] to extract the visual object concept “mascot” in Case 4 can also be regarded as a way of implicitly using external knowledge, this knowledge is not fine-grained and accurate enough compared to “Mario” and “Luigi”.

We also visualize some negative examples generated by our

model on TextCaps validation dataset in Fig. 7. In Case a, strong baseline CNMT simply depicts the characters on the dial. In contrast, our model attempts to generate higher-level information, namely time. However, our model reads the time of the watch incorrectly. We consider the reason is that the ability of DEVICE to model the relationship between objects and scene text is still limited. Besides, it is difficult for models to read the time on the dial without numbers. In Case b, CNMT and DEVICE cannot correctly capture the information of “measuring length”, which shows that current models are generally less capable of perceiving intent in scenes.

V. CONCLUSION

In this paper, we propose a DEpth and VISual ConcEpts Aware Transformer (DEVICE) for TextCaps, which is capable of generating accurate and comprehensive captions for given images. We introduce depth information and design a depth-enhanced feature updating module to improve OCR appearance features, which is capable of facilitating the construction of 3D geometric relations. Meanwhile, we introduce the semantic information of salient visual object concepts and propose a semantic-guided alignment module to interact visual concepts with aligned scene text, which improves the integrity of captions. More remarkably, our model achieves state-of-the-art performances on the TextCaps test set. By comparing experimental results with human annotations, we consider that extracting more explicit external knowledge can further improve this task.

REFERENCES

- [1] P. Anderson, X. He, C. Buehler, D. Teney, M. Johnson, S. Gould, and L. Zhang, “Bottom-up and top-down attention for image captioning and visual question answering,” in *Proceedings of the IEEE conference on computer vision and pattern recognition*, 2018, pp. 6077–6086. **1, 2, 6, 7**
- [2] Z. Zhang, Q. Wu, Y. Wang, and F. Chen, “High-quality image captioning with fine-grained and semantic-guided visual attention,” *IEEE Transactions on Multimedia*, vol. 21, no. 7, pp. 1681–1693, 2018. **1**
- [3] L. Yu, J. Zhang, and Q. Wu, “Dual attention on pyramid feature maps for image captioning,” *IEEE Transactions on Multimedia*, vol. 24, pp. 1775–1786, 2021. **1**
- [4] O. Sidorov, R. Hu, M. Rohrbach, and A. Singh, “Textcaps: a dataset for image captioning with reading comprehension,” in *European conference on computer vision*. Springer, 2020, pp. 742–758. **1, 2, 4, 5, 6, 7, 8**
- [5] F. Borisyuk, A. Gordo, and V. Sivakumar, “Rosetta: Large scale system for text detection and recognition in images,” in *Proceedings of the 24th ACM SIGKDD international conference on knowledge discovery & data mining*, 2018, pp. 71–79. **1, 3, 6**
- [6] Z. Wang, R. Bao, Q. Wu, and S. Liu, “Confidence-aware non-repetitive multimodal transformers for textcaps,” in *Proceedings of the AAAI Conference on Artificial Intelligence*, vol. 35, no. 4, 2021, pp. 2835–2843. **1, 2, 4, 6, 7, 8, 9**
- [7] J. Wang, J. Tang, and J. Luo, “Multimodal attention with image text spatial relationship for ocr-based image captioning,” in *Proceedings of the 28th ACM International Conference on Multimedia*, 2020, pp. 4337–4345. **1, 2, 6, 7**
- [8] J. Wang, J. Tang, M. Yang, X. Bai, and J. Luo, “Improving ocr-based image captioning by incorporating geometrical relationship,” in *Proceedings of the IEEE/CVF conference on computer vision and pattern recognition*, 2021, pp. 1306–1315. **1, 2, 3, 6, 7, 8**
- [9] Z. Yang, Y. Lu, J. Wang, X. Yin, D. Florencio, L. Wang, C. Zhang, L. Zhang, and J. Luo, “Tap: Text-aware pre-training for text-vqa and text-caption,” in *Proceedings of the IEEE/CVF conference on computer vision and pattern recognition*, 2021, pp. 8751–8761. **2, 7, 8**
- [10] J. H. Lee, M.-K. Han, D. W. Ko, and I. H. Suh, “From big to small: Multi-scale local planar guidance for monocular depth estimation,” *arXiv preprint arXiv:1907.10326*, 2019. **2, 3**
- [11] A. Radford, J. W. Kim, C. Hallacy, A. Ramesh, G. Goh, S. Agarwal, G. Sastry, A. Askell, P. Mishkin, J. Clark *et al.*, “Learning transferable visual models from natural language supervision,” in *International Conference on Machine Learning*. PMLR, 2021, pp. 8748–8763. **2, 3, 5, 6, 9**
- [12] O. Vinyals, A. Toshev, S. Bengio, and D. Erhan, “Show and tell: A neural image caption generator,” in *Proceedings of the IEEE conference on computer vision and pattern recognition*, 2015, pp. 3156–3164. **2**
- [13] L. Huang, W. Wang, J. Chen, and X.-Y. Wei, “Attention on attention for image captioning,” in *Proceedings of the IEEE/CVF international conference on computer vision*, 2019, pp. 4634–4643. **2, 6, 7**
- [14] Q. Huang, Y. Liang, J. Wei, Y. Cai, H. Liang, H.-f. Leung, and Q. Li, “Image difference captioning with instance-level fine-grained feature representation,” *IEEE Transactions on Multimedia*, vol. 24, pp. 2004–2017, 2021. **2**
- [15] M. Cornia, M. Stefanini, L. Baraldi, and R. Cucchiara, “Meshed-memory transformer for image captioning,” in *Proceedings of the IEEE/CVF conference on computer vision and pattern recognition*, 2020, pp. 10578–10587. **2**
- [16] A. Vaswani, N. Shazeer, N. Parmar, J. Uszkoreit, L. Jones, A. N. Gomez, L. Kaiser, and I. Polosukhin, “Attention is all you need,” *Advances in neural information processing systems*, vol. 30, 2017. **2, 5**
- [17] A. Singh, V. Natarajan, M. Shah, Y. Jiang, X. Chen, D. Batra, D. Parikh, and M. Rohrbach, “Towards vqa models that can read,” in *Proceedings of the IEEE/CVF conference on computer vision and pattern recognition*, 2019, pp. 8317–8326. **2, 7**
- [18] A. F. Biten, R. Litman, Y. Xie, S. Appalaraju, and R. Manmatha, “Latr: Layout-aware transformer for scene-text vqa,” in *Proceedings of the IEEE/CVF Conference on Computer Vision and Pattern Recognition*, 2022, pp. 16548–16558. **2**
- [19] Z.-X. Jin, M. Z. Shou, F. Zhou, S. Tsutsui, J. Qin, and X.-C. Yin, “From token to word: Ocr token evolution via contrastive learning and semantic matching for text-vqa,” in *Proceedings of the 30th ACM International Conference on Multimedia*, 2022, pp. 4564–4572. **2**
- [20] G. Zeng, Y. Zhang, Y. Zhou, and X. Yang, “Beyond ocr+ vqa: involving ocr into the flow for robust and accurate textvqa,” in *Proceedings of the 29th ACM International Conference on Multimedia*, 2021, pp. 376–385. **2**
- [21] R. Hu, A. Singh, T. Darrell, and M. Rohrbach, “Iterative answer prediction with pointer-augmented multimodal transformers for textvqa,” in *Proceedings of the IEEE/CVF Conference on Computer Vision and Pattern Recognition*, 2020, pp. 9992–10002. **2, 4**
- [22] W. Zhang, H. Shi, J. Guo, S. Zhang, Q. Cai, J. Li, S. Luo, and Y. Zhuang, “Magic: Multimodal relational graph adversarial inference for diverse and unpaired text-based image captioning,” in *Proceedings of the AAAI Conference on Artificial Intelligence*, vol. 36, no. 3, 2022, pp. 3335–3343. **2, 6, 7**
- [23] G. Xu, S. Niu, M. Tan, Y. Luo, Q. Du, and Q. Wu, “Towards accurate text-based image captioning with content diversity exploration,” in *Proceedings of the IEEE/CVF Conference on Computer Vision and Pattern Recognition*, 2021, pp. 12637–12646. **2, 6, 7**
- [24] W. Tang, Z. Hu, Z. Song, and R. Hong, “Ocr-oriented master object for text image captioning,” in *Proceedings of the 2022 International Conference on Multimedia Retrieval*, 2022, pp. 39–43. **2, 6, 7**
- [25] C. Couprie, C. Farabet, L. Najman, and Y. LeCun, “Indoor semantic segmentation using depth information,” *arXiv preprint arXiv:1301.3572*, 2013. **2**
- [26] A. Geiger, P. Lenz, and R. Urtasun, “Are we ready for autonomous driving? the kitti vision benchmark suite,” in *2012 IEEE conference on computer vision and pattern recognition*. IEEE, 2012, pp. 3354–3361. **2**
- [27] P. Banerjee, T. Gokhale, Y. Yang, and C. Baral, “Weakly supervised relative spatial reasoning for visual question answering,” in *Proceedings of the IEEE/CVF International Conference on Computer Vision*, 2021, pp. 1908–1918. **2**
- [28] Z. Wang, Y. Luo, Y. Li, Z. Huang, and H. Yin, “Look deeper see richer: Depth-aware image paragraph captioning,” in *Proceedings of the 26th ACM international conference on Multimedia*, 2018, pp. 672–680. **2**
- [29] Z. Liao, Q. Huang, Y. Liang, M. Fu, Y. Cai, and Q. Li, “Scene graph with 3d information for change captioning,” in *Proceedings of the 29th ACM International Conference on Multimedia*, 2021, pp. 5074–5082. **2**
- [30] Y. Liu, W. Wei, D. Peng, X.-L. Mao, Z. He, and P. Zhou, “Depth-aware and semantic guided relational attention network for visual question answering,” *IEEE Transactions on Multimedia*, pp. 1–14, 2022. **2**
- [31] Y. Qiu, Y. Satoh, R. Suzuki, K. Iwata, and H. Kataoka, “3d-aware scene change captioning from multiview images,” *IEEE Robotics and Automation Letters*, vol. 5, no. 3, pp. 4743–4750, 2020. **2**

- [32] S. Ren, K. He, R. Girshick, and J. Sun, "Faster r-cnn: Towards real-time object detection with region proposal networks," *Advances in neural information processing systems*, vol. 28, 2015. 3
- [33] Googleocr, <https://cloud.google.com/functions/docs/tutorials/ocr>. 3, 6
- [34] P. Bojanowski, E. Grave, A. Joulin, and T. Mikolov, "Enriching word vectors with subword information," *Transactions of the association for computational linguistics*, vol. 5, pp. 135–146, 2017. 4, 5
- [35] J. Almazán, A. Gordo, A. Fornés, and E. Valveny, "Word spotting and recognition with embedded attributes," *IEEE transactions on pattern analysis and machine intelligence*, vol. 36, no. 12, pp. 2552–2566, 2014. 4
- [36] H.-H. Wu, P. Seetharaman, K. Kumar, and J. P. Bello, "Wav2clip: Learning robust audio representations from clip," in *ICASSP 2022-2022 IEEE International Conference on Acoustics, Speech and Signal Processing (ICASSP)*. IEEE, 2022, pp. 4563–4567. 5
- [37] R. Zhang, Z. Guo, W. Zhang, K. Li, X. Miao, B. Cui, Y. Qiao, P. Gao, and H. Li, "Pointclip: Point cloud understanding by clip," in *Proceedings of the IEEE/CVF Conference on Computer Vision and Pattern Recognition*, 2022, pp. 8552–8562. 5
- [38] Y. Ma, G. Xu, X. Sun, M. Yan, J. Zhang, and R. Ji, "X-clip: End-to-end multi-grained contrastive learning for video-text retrieval," in *Proceedings of the 30th ACM International Conference on Multimedia*, 2022, pp. 638–647. 5
- [39] O. Vinyals, M. Fortunato, and N. Jaitly, "Pointer networks," *Advances in neural information processing systems*, vol. 28, 2015. 6
- [40] K. Papineni, S. Roukos, T. Ward, and W.-J. Zhu, "Bleu: a method for automatic evaluation of machine translation," in *Proceedings of the 40th annual meeting of the Association for Computational Linguistics*, 2002, pp. 311–318. 6
- [41] M. Liao, B. Shi, X. Bai, X. Wang, and W. Liu, "Textboxes: A fast text detector with a single deep neural network," in *Thirty-first AAAI conference on artificial intelligence*, 2017. 6
- [42] S. Banerjee and A. Lavie, "Meteor: An automatic metric for mt evaluation with improved correlation with human judgments," in *Proceedings of the acl workshop on intrinsic and extrinsic evaluation measures for machine translation and/or summarization*, 2005, pp. 65–72. 6
- [43] P. Anderson, B. Fernando, M. Johnson, and S. Gould, "Spice: Semantic propositional image caption evaluation," in *European conference on computer vision*. Springer, 2016, pp. 382–398. 6
- [44] R. Vedantam, C. Lawrence Zitnick, and D. Parikh, "Cider: Consensus-based image description evaluation," in *Proceedings of the IEEE conference on computer vision and pattern recognition*, 2015, pp. 4566–4575. 6
- [45] Q. Zhu, C. Gao, P. Wang, and Q. Wu, "Simple is not easy: A simple strong baseline for textvqa and textcaps," in *Proceedings of the AAAI Conference on Artificial Intelligence*, vol. 35, no. 4, 2021, pp. 3608–3615. 6, 7, 8
- [46] N. Wang, J. Xie, J. Wu, M. Jia, and L. Li, "Controllable image captioning via prompting," *arXiv preprint arXiv:2212.01803*, 2022. 7
- [47] J. Devlin, M.-W. Chang, K. Lee, and K. Toutanova, "Bert: Pre-training of deep bidirectional transformers for language understanding," *arXiv preprint arXiv:1810.04805*, 2018. 6
- [48] A. Kingma, "A method for stochastic optimization," *Anon. International Conference on Learning Representations. San Diego: ICLR*, 2015. 6
- [49] A. F. Biten, R. Tito, A. Mafla, L. Gomez, M. Rusinol, E. Valveny, C. Jawahar, and D. Karatzas, "Scene text visual question answering," in *Proceedings of the IEEE/CVF international conference on computer vision*, 2019, pp. 4291–4301. 7
- [50] R. Krishna, Y. Zhu, O. Groth, J. Johnson, K. Hata, J. Kravitz, S. Chen, Y. Kalantidis, L.-J. Li, D. A. Shamma *et al.*, "Visual genome: Connecting language and vision using crowdsourced dense image annotations," *International journal of computer vision*, vol. 123, pp. 32–73, 2017. 7
- [51] T.-Y. Lin, M. Maire, S. Belongie, J. Hays, P. Perona, D. Ramanan, P. Dollár, and C. L. Zitnick, "Microsoft coco: Common objects in context," in *Computer Vision—ECCV 2014: 13th European Conference, Zurich, Switzerland, September 6-12, 2014, Proceedings, Part V 13*. Springer, 2014, pp. 740–755. 7
- [52] P. Sharma, N. Ding, S. Goodman, and R. Soicrut, "Conceptual captions: A cleaned, hypernymed, image alt-text dataset for automatic image captioning," in *Proceedings of the 56th Annual Meeting of the Association for Computational Linguistics (Volume 1: Long Papers)*, 2018, pp. 2556–2565. 7
- [53] V. Ordonez, G. Kulkarni, and T. Berg, "Im2text: Describing images using 1 million captioned photographs," *Advances in neural information processing systems*, vol. 24, 2011. 7
- [54] C. Schuhmann, R. Vencu, R. Beaumont, R. Kaczmarczyk, C. Mullis, A. Katta, T. Coombes, J. Jitsev, and A. Komatsuzaki, "Laion-400m: Open dataset of clip-filtered 400 million image-text pairs," *arXiv preprint arXiv:2111.02114*, 2021. 7